JOURNAL OF MATERIALS SCIENCE 21 (1986) 2100–2108

Blue a.c. electroluminescence of $Zn_{1-x}Mg_xS$:Cu,Br powder phosphors

R. REVATHI, T. R. N. KUTTY*
Materials Research Laboratory, Indian Institute of Science, Bangalore 560 012, India

Blue a.c. electroluminescent (EL) powder phosphors with brightness of ~300 Cd/m^2 and half life of over 10^3 h can be prepared from $Zn_{1-x}Mg_xS$:Cu,Br. Replacement of zinc by the more electropositive magnesium increases the percentage ionicity of metal–sulphur bonds leading to the stabilization of the 2H structure. Incorporation of 15 mol% Mg shifts the EL emission peak from 525 to 436 nm. The green side band is completely absent when the copper concentration is ~0.3 mol%. When copper is ~10^{-4} mol%, both the green and blue bands are observed in the photoluminescence (PL) emission spectrum. It is proposed that hexagonal $Zn_{1-x}Mg_xS$ with 0.3 mol% copper contains predominantly ($Cu^-_{Zn}Cu^+_i$) pairs due to increased electrostatic energy. The recombination involving this isoelectronic hole centre and an isolated donor produces the blue emission. Since a large fraction of the acceptor is present as independent Cu^-_{Zn} at low copper concentrations, the green band persists, which originates from distant donor (Br^+_S)–acceptor (Cu^-_{Zn}) pairs.

1. Introduction

It has been found that a.c. electroluminescent ZnS powder phosphors emitting green light have longer life times [1–5], whereas stable blue EL phosphors are difficult to prepare. Short living ZnS:Cu,Cl has blue EL when the chlorine concentration is low and copper/chlorine > 1 are maintained; the blue emission is always accompanied by a green side band [6]. ZnS:Cu,I and ZnS:Cu,Al also show blue EL; the former has a short half-life, while the latter does not emit saturated blue due to the weak orange side band [7, 8]. ZnS:Ag,Cu,Al phosphor shows low intensity blue EL [9]. It is, therefore, necessary to look for modified ZnS or other lattices for preparing stable blue EL powder phosphors. Jaffe [10] reported blue EL in $Zn_{1-x}Mg_xS$:Cu,halogen phosphors. After this early work, there are no reports on this system till Fischer [11] observed that blue EL phosphors of better stability can be prepared from $Zn_{1-x}Mg_xS$.

The ZnS–MgS system has been worked out by many authors [12–18], mostly using single crystals. ZnS has a generally accepted phase transformation around 1020° C, from 3C to 2H structure, whereas MgS has a rock salt structure. The limit of MgS solubility in ZnS is ~49 mol% for single crystals grown from the melt [12–16]. The powder material formed by the reaction of ZnS and MgO with CS_2 vapour at 1050° C has the solubility limit of 22 mol% MgS [17]. $Zn_{1-x}Mg_xS$ prepared from molten $ZnCl_2$ + $MgCl_2$ in H_2S at 800° C showed higher solubility of ~30 mol% MgS [18]. In these powder materials, the presence of > 10 mol% MgS inhibits the formation of the 3C phase, down to room temperature. In the range of $0 < x < 0.11$, $Zn_{1-x}Mg_xS$ crystals have the 3C structure with hexagonal stacking faults [16]. Regarding the stability range of the cubic and hexagonal phases with composition, it is possible that most of the authors [12–18] may be dealing with non-equilibrium materials.

Cathodoluminescence of copper-activated $Zn_{1-x}Mg_xS$ phosphors showed limited shift in emission maximum with increasing magnesium content [19]. This seemed peculiar since the band gap energy (E_g) of MgS (≃4.8 eV) is much larger than that of ZnS (~3.7 eV). Kroeger [20] reported that the incorporation of MgS in ZnS does not introduce any new levels in the forbidden gap and hence there are no observable changes in the luminescence of ZnS with magnesium incorporation. The present work revealed that the EL emission maximum shifts from 525 nm for ZnS:Cu,Br to 436 nm for $Zn_{0.85}Mg_{0.15}S$:Cu,Br. We also observed that the variations in EL spectra can be correlated to the crystallochemical changes in $Zn_{1-x}Mg_xS$.

2. Experimental details

The molten salt technique, as in [18], could not be adopted for controlled addition of halogen in the phosphors; hence the solid state reaction was used. ZnS was of luminescence grade from General Electric, Schenectady, New York, USA. MgS was prepared by firing $MgCO_3$ at 800° C in H_2S for 2 h. The solid solubility limit was determined chemically by hydrolysis, whereupon the H_2S liberated was quantitatively estimated. Only free MgS, if present, gave rise to H_2S, whereas $Zn_{1-x}Mg_xS$ remained unreacted [10, 19, 21]. X-ray powder diffraction patterns confirmed the chemical tests.

* *Permanent address*: Department of Inorganic and Physical Chemistry, Indian Institute of Science, Bangalore, India.

0022–2461/86 $03.00 + .12

$Zn_{1-x}Mg_xS$:Cu,Br phosphors were prepared by slurrying ZnS with copper-acetate and NH_4Br in water, drying at 120° C and mixing with the required amount of MgS and 1% wt elemental sulphur. ZnS and $Mg(OH)_2MgCO_3$ could also be used as the starting materials. Magnesium content was varied from 0 to 25 mol %, whereas copper and bromine ranges from 0.5 to 3 and 0.2 to 4 mol % respectively, in the starting material. After drying, the powder was heated to 800° C in H_2S for 1 h and then in pure N_2 for 2 h. The samples were fired in silica tubes capped with silica wool and were contained in a larger silica tube closed at one end and having a gas inlet and outlet at the other end. The phosphor was quenched to room temperature. Excess $Cu_{2-\delta}S$ (δ = 0.002 to 0.2) was dissolved away by washing in 10% KCN + KOH solution. The phosphor was reheated at 700° C for 1 h and cooled fast by dipping the outer tube in water. Copper and bromine in the KCN-washed samples were determined by atomic adsorption spectrophotometry and colorimetry respectively.

EL panels (35–50 μm thick) were prepared by spreading the powder (5–12 μm grain size) on ITO (indium oxide doped with tin oxide, $In_2O_3:SnO_2$) glass plates carrying cyanoethyl starch + cyanoethyl sucrose (dielectric constant $\varepsilon \sim 20$) or polyvinylidene fluoride ($\varepsilon \sim 9$) coatings. The back electrodes were evaporated aluminium. EL a.c. measurements were carried out in dry atmosphere using a brightness spotmeter (Photo Research, Burbank, California). EL emission spectra were recorded with a Schoeffel monochromator coupled with a photodetector. An Hitachi 650–40 fluorescence spectrophotometer recorded the photoluminescence (PL) emission and excitation spectra. A Shimadzu spectrophotometer was used for optical reflectance spectra. X-ray powder patterns were obtained with a Philips PW 1700 diffractometer. Proper care was taken to eliminate the moisture during the diffraction experiments. Lattice parameters were measured for the cubic phase in the range of 2θ = 87.9–88.5° ((4 2 2) reflection), with Cu$K\alpha$ radiation (θ = Bragg angle), using silicon as the internal standard. For the hexagonal phase (2 0 3) and (2 1 3) reflections (2θ = 72.95 and 91.91°, respectively) were used for lattice parameter determinations.

3. Results

3.1. Solubility limits

Hydrolysis experiments showed that free MgS is present when $x > 0.24$ for $Zn_{1-x}Mg_xS$ fired at 800° C. At 950° C, this limit increases to 0.26, indicating the enhanced solubility of MgS in ZnS with temperature. This observed solubility limit is nearly in agreement with the earlier reports on powder materials [10, 17–19]. $Zn_{1-x}Mg_xS$ prepared by the solid state method has lower solubility limits than that from the fused salt method [18]. However the lower solubility is not due to the formation of MgO as evident from the chemical analysis and the absence of MgO reflections in the X-ray diffractograms. $MgCO_3$ at 800° C will decompose rapidly to MgO which is normally unreactive to H_2S and elemental sulphur. If the reactants are initially completely free of moisture, we found that the nascent oxide produced *in situ* by the decomposition of $MgCO_3$ converts to the sulphide phase.

3.2. Crystallographic changes

X-ray powder diffractograms of $Zn_{1-x}Mg_xS$, within the homogeneity range, showed that ZnS gradually transforms from 3C to 2H as magnesium content is increased (Fig. 1). X-ray reflections at 2θ = 26.9, 31.5 and 39.5° (Cu$K\alpha$ radiation) arise only from the 2H phase, while reflection at 2θ = 33.05° is from the 3C phase only. The intensity ratios, $I_{26.9}/I_{33.05}$ and $I_{39.5}/I_{33.05}$ are proportional to the hexagonal phase content. X-ray reflections due to the 3C phase disappear when $x \simeq 0.13$. Calibration curves for hexagonality against intensity ratio are obtained from the mechanical mixtures of 100% 3C and 2H forms prepared by independent methods, in known proportions. Since the 3C to 2H transformation is around 1020° C and is reversible for pure ZnS, the above changes are due to magnesium substitution. Extended annealing in a vacuum (10^{-6} atm) for 6 to 8 days at 800° C has not changed the phase content of $Zn_{0.87}Mg_{0.13}S$. Apparently, the 2H phase is thermodynamically stable, though extended kinetic stability cannot be ruled out. Copper and bromine, within the concentration ranges mentioned later, are found to have only a marginal influence on Fig. 1. Although $Cu_{2-\delta}S$ has the tendency to stabilize the cubic form of ZnS [22, 23], it does not seem to influence the phase content in $Zn_{1-x}Mg_xS$.

For both 3C and 2H phases, the unit cell parameters increase with magnesium content. ZnS fired at 800° C in H_2S has a_0^{cub} = 0.54095 nm which agrees with the reported value [24]. a_0^{cub} increases to 0.54125 nm when $x \simeq 0.06$. For the 2H phase, a_0^{hex} and c_0^{hex} increase non-linearly with magnesium content (Fig. 2). a_0^{hex} values are closer to those reported for $Zn_{1-x}Mg_xS$

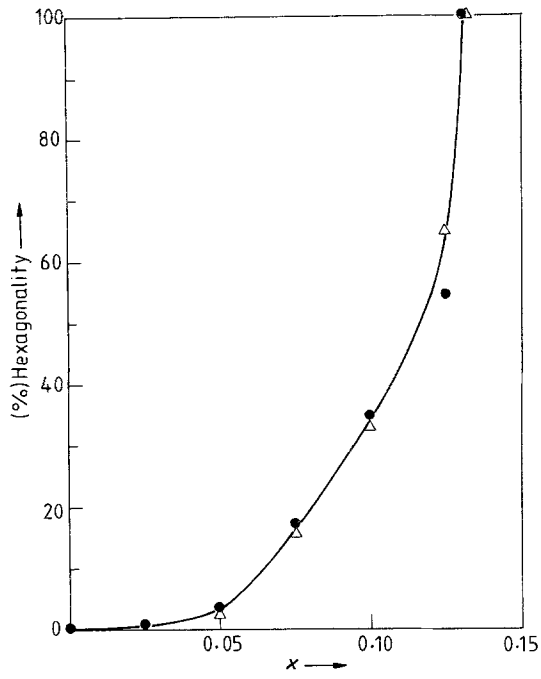

Figure 1 Percentage hexagonality of $Zn_{1-x}Mg_xS$ solid solutions as a function of x-values. (●) represents hexagonality calculated from $I_{26.9}/I_{33.1}$ whereas (△) represents those calculated from $I_{39.5}/I_{33.1}$ ratios.

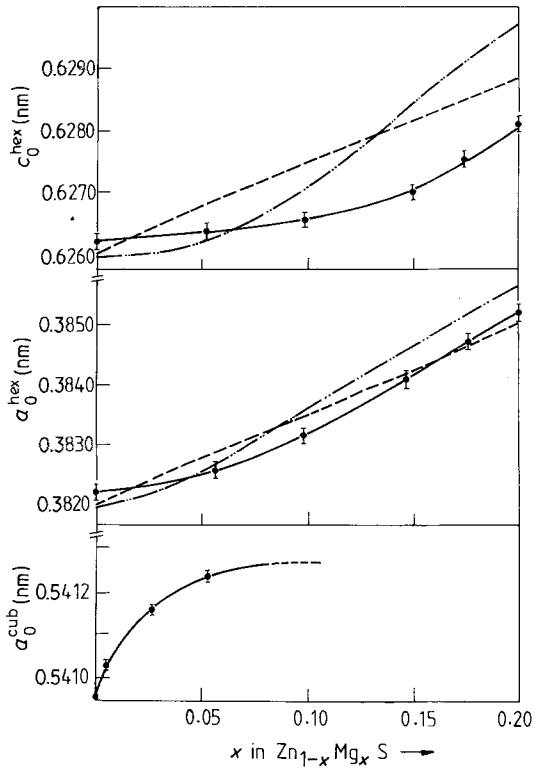

Figure 2 The variation in lattice parameters of cubic and hexagonal phases of $Zn_{1-x}Mg_xS$ with composition. The full lines represent the observed values from this work. Dashed lines are obtained by the interpolation of 2H ZnS [25] and 2H MgS [26] lattice parameters. The dotted lines are those reported for single crystals [12].

single crystals [12], whereas c_0^{hex} values are somewhat lower, particularly at higher x-values. Similar trends have been noticed for $Zn_{1-x}Mg_xS$ powder prepared from molten salts [18]. Fig. 2 indicates that the incorporation of magnesium expands the ZnS lattice. Assuming linear dependence of a_0^{hex} and c_0^{hex} values on composition, straight lines are drawn in Fig. 2, using the cell parameters of 2H ZnS [25] and of the wurtzite form of MgS [26]. The observed cell parameters deviate from the linear compositional curves indicating the non-ideal nature of the solid solutions. Again, copper and bromine, within the concentration ranges mentioned subsequently, do not alter the cell parameters (within 1%).

3.3. Electroluminescence characteristics

Fig. 3 shows the EL spectrum of $Zn_{0.82}Mg_{0.18}S$:0.3 Cu, 0.35 Br (composition of the dopants in the KCN-washed phosphors) at room temperature. The emission maximum is around 436 nm. For 3C ZnS, with the same concentrations of dopants, the EL emission maximum is at 525 nm. On increasing the copper/bromine ratio, the EL spectrum of ZnS shifts to blue ($\lambda_{max} \simeq 460$ nm). However, there is a green side band for this spectrum (Fig. 3b). For $Zn_{1-x}Mg_xS$:Cu,Br, with $x > 0.13$, the green band is not observed for a range of copper/bromine ratio (0.4–3.0). However the green band appears when the copper concentration is less than 10^{-2} mol %. The EL intensities of phosphors with lower copper contents are considerably low. Both the green and blue bands are present in the EL spectrum of $Zn_{1-x}Mg_xS$:Cu,Br with $0.05 < x < 0.13$. The variations in EL emission maxima of these two

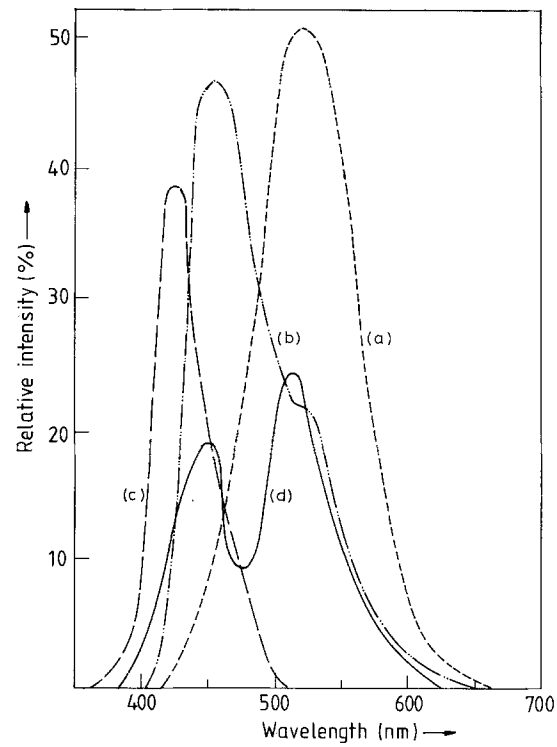

Figure 3 Electroluminescence spectra of (a) ZnS:0.3Cu,0.35Br, (b) ZnS:0.3Cu,0.2Br, (c) $Zn_{0.82}Mg_{0.18}S$:0.3Cu,0.35Br and (d) $Zn_{0.92}Mg_{0.08}S$:0.3Cu,0.3Br (2.5 kHz).

bands with magnesium content are shown in Fig. 4. The corresponding changes in their relative intensities are also shown in the same figure. While the intensity of the green band goes down to zero for $x \geqslant 0.13$, that of the blue band is maximum at $x \geqslant 0.18$.

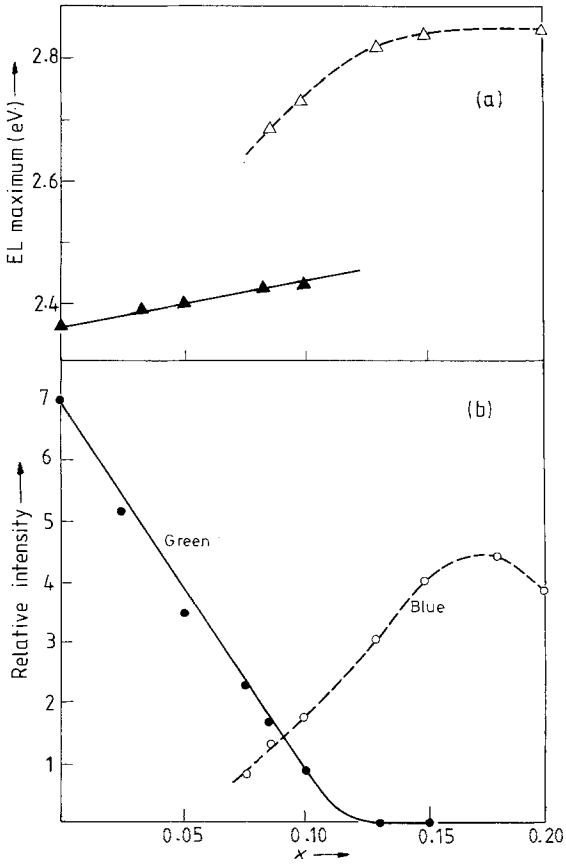

Figure 4 EL characteristics as a function of composition for $Zn_{1-x}Mg_xS$:0.3Cu,0.3Br. Variation in (a) EL emission maximum and (b) the intensity for the green and blue bands.

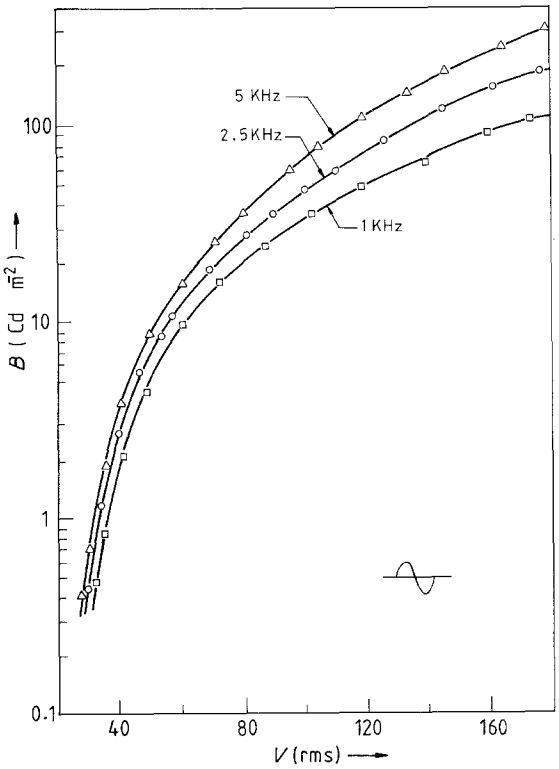

Figure 5 Brightness (B)–Voltage (V) relation for $Zn_{0.85}Mg_{0.15}S$: 0.3Cu,0.3Br for different frequencies of operation.

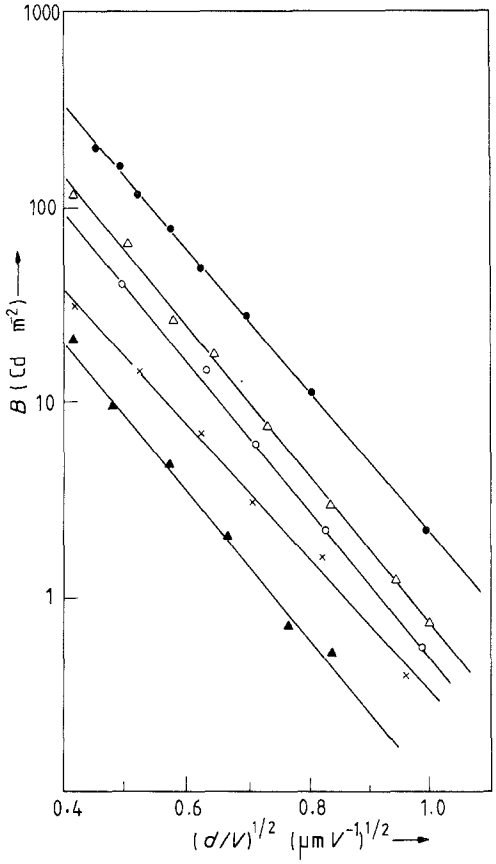

Figure 6 A plot of $(d/V)^{1/2}$ as a function of brightness, where d is expressed in μm and V in volts, for $Zn_{1-x}Mg_xS$:0.3Cu,0.3Br phosphors of varying x values. Brightness corresponds to the combined intensities of the green and the blue bands. (●) $x = 0.02$, (△) $x = 0.15$, (○) $x = 0.05$, (x) $x = 0.06$, (▲) $x = 0.10$.

Brightness (B)–voltage (V) curves for blue EL of $Zn_{0.85}Mg_{0.15}S$:0.3Cu,0.3Br indicate no apparent saturation with frequency of operation (Fig. 5). The EL intensity increases with frequency without a shift in the emission maximum. Brightness also increases with voltage, at fixed frequency. A plot of $(d/V)^{1/2}$ against $\log B$, where d is the thickness of the EL layer, gives straight lines (Fig. 6). The combined EL brightness (of the green and blue bands together) decreases with x values till ~ 0.1 and further increases, reaching the upper limit at $x \simeq 0.18$. It is reported that $Zn_{1-x}Mg_xS$ has considerable hexagonal stacking faults when $x < 0.11$ [16]. There may be other types of stacking faults when $Zn_{1-x}Mg_xS$ approaches the solubility limits ($x = 0.24$). Radiationless recombinations involving these defects decrease the luminescence efficiency. This explains the variations in EL intensity with x-values (Figs 4 and 6).

The relationship between brightness B and time, t, at constant operational voltage and frequency, is given by [5]:

$$B = B_0/[1 + (t/\tau)^n] \qquad (1)$$

where B is the brightness at any time t, B_0 is the initial brightness and n is a number greater than unity. The intersection of $(B_0/B - 1) = 1$ indicates the half-life, (τ). Phosphors annealed under special conditions at 700° C have $\tau = 1.2 \times 10^3$ h whereas those without the annealing have half-life around 150 h (Fig. 7).

3.4. Optical reflectance spectrum

Optical reflectance spectra of $Zn_{1-x}Mg_xS$ are recorded in the range of 250 to 850 nm at liquid N_2 temperature (−196° C). Since the spectra are somewhat broad, we resorted to the McClean [27] equation to derive the band gap energy, E_g:

$$\alpha h\nu = K(h\nu - E_g \pm E_p)^{1/n} \qquad (2)$$

where E_p is the energy of the associated phonon, K is the proportionality constant, h is Planck's constant and ν is the frequency; $n = 2$ for direct allowed transition. Alternatively, transformation of the McClean equation to the Kubelka–Munk function [28] is carried out:

$$\alpha = sF(R_\infty),$$

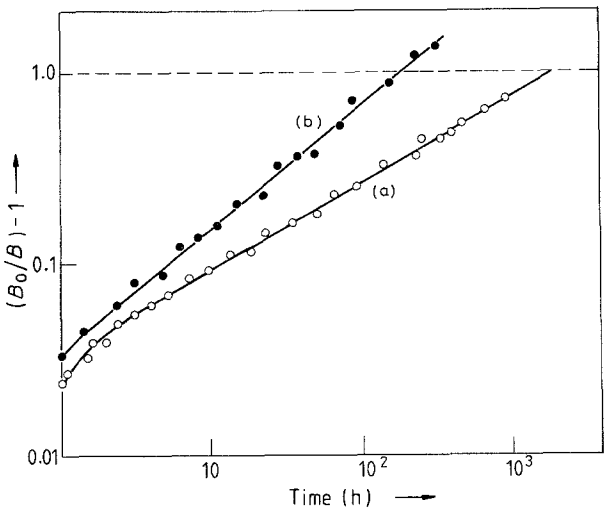

Figure 7 Time dependence of brightness for $Zn_{0.82}Mg_{0.18}S$:0.3Cu, 0.35Br as per Equation 1: (a) for the annealed and (b) for the unannealed phosphor (1 kHz, 110 V).

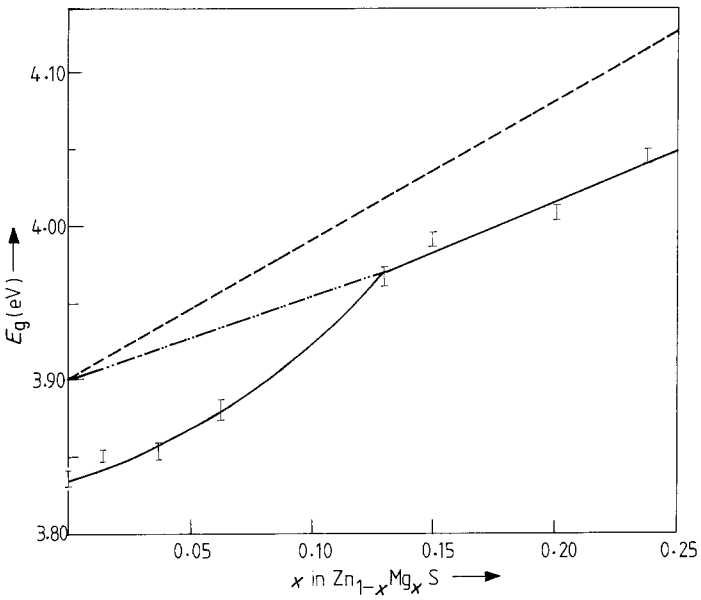

Figure 8 Variation in E_g values with composition at $-196°$ C. The dashed line is as per Equation 4 whereas the curved line is calculated from Equation 5.

where α is the absorption coefficient, F is a functional constant and R is the reflectivity at the angle of incidence θ or ∞; this yields

$$sF(R_\theta)h\nu = K(h\nu - E_g \pm E_p) \quad (3)$$

where s, the scattering function, is assumed to be independent of wavelength. Fig. 8 shows the variation in E_g values with magnesium content, within the solubility limits of MgS in ZnS. For samples with mixed 3C + 2H phases ($0.06 < x < 0.12$), the reflectance spectra are so broad that the E_g values are not accurately measurable. The large width of the spectra may arise from the high stacking fault concentration [13–16]. For the hexagonal form of MgS, E_{g_1} is estimated around 4.8 eV [16], whereas for 2H ZnS it is around 3.91 eV [29]. The observed E_g values for $Zn_{1-x}Mg_xS$ deviate from the linear curve. They fall as a parabolic curve represented by:

$$E_g = E_{g_2} + [E_{g_1} - E_{g_2} - b]x + bx^2 \quad (4)$$

where the calculated bowing parameter, b, is $\simeq 0.40$ eV. When $x < 0.06$, the observed band gap energy values follow another parabolic curve where $E_{g_2} \simeq 3.83$ eV, corresponding to that of 3C ZnS [29]. Reflectance spectra around room temperature indicate that the temperature coefficient of E_g value is $\sim 6 \times 10^{-4}$ eV° C^{-1} for the hexagonal $Zn_{1-x}Mg_xS$.

Investigations of Fedorov *et al.* [16] on the reflectance spectra of $Zn_{1-x}Mg_xS$ single crystal at liquid helium temperature revealed the existence of three exciton transitions. We could not observe the exciton lines with the powder samples at liquid N_2 temperature. This may be due to the surface effects in polycrystalline samples. However, PL excitation spectra of copper-doped $Zn_{1-x}Mg_xS$ phosphors showed some exciton structures.

3.5. Photoluminescence spectra

Incorporation of magnesium may not basically change the EL excitation mechanism prevailing in ZnS:Cu,Br whereas the emission process may be altered. PL studies yield definite information regarding the emission mechanism, particularly since the PL emission spectra of $Zn_{1-x}Mg_xS$:Cu,Br have good resemblance to those of EL emission (compare Figs. 4 and 9).

Fig. 9 shows the emission and excitation spectra for $Zn_{0.85}Mg_{0.15}S$:0.3Cu,0.35Br at $-196°$ C. The emission spectrum consists of only one band, with $\lambda_{max} = 432$ nm. It has lower half-band width than that of copper-blue emission band in ZnS. The emission maximum shifts to lower energy with temperture, as in the case of copper-blue and copper-green in ZnS. However, the half-band width decreases with temperature, a trend opposite to that observed for copper-blue in ZnS [30]. The emission spectrum does not

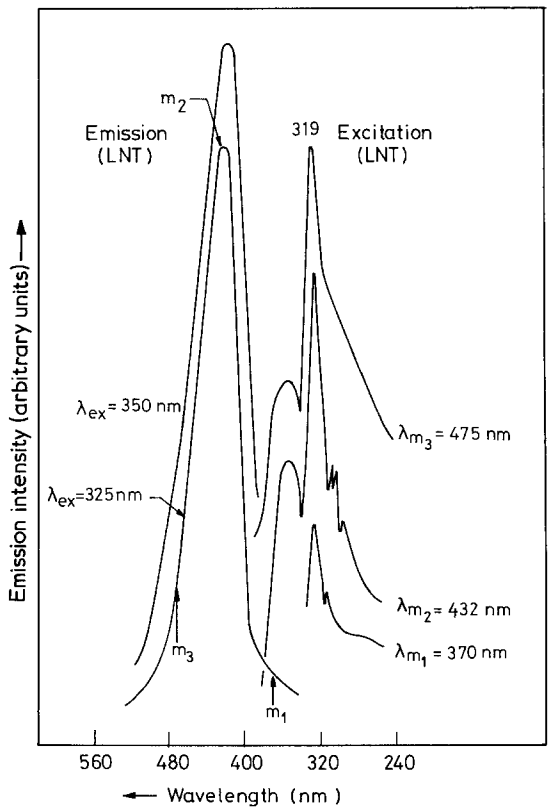

Figure 9 Emission and excitation spectra for $Zn_{0.85}Mg_{0.15}S$:0.3Cu, 0.35Br at $-196°$ C. λ_m represents the monitored wavelength for excitation spectrum and λ_{ex} indicates the exciting wavelength for the emission spectrum.

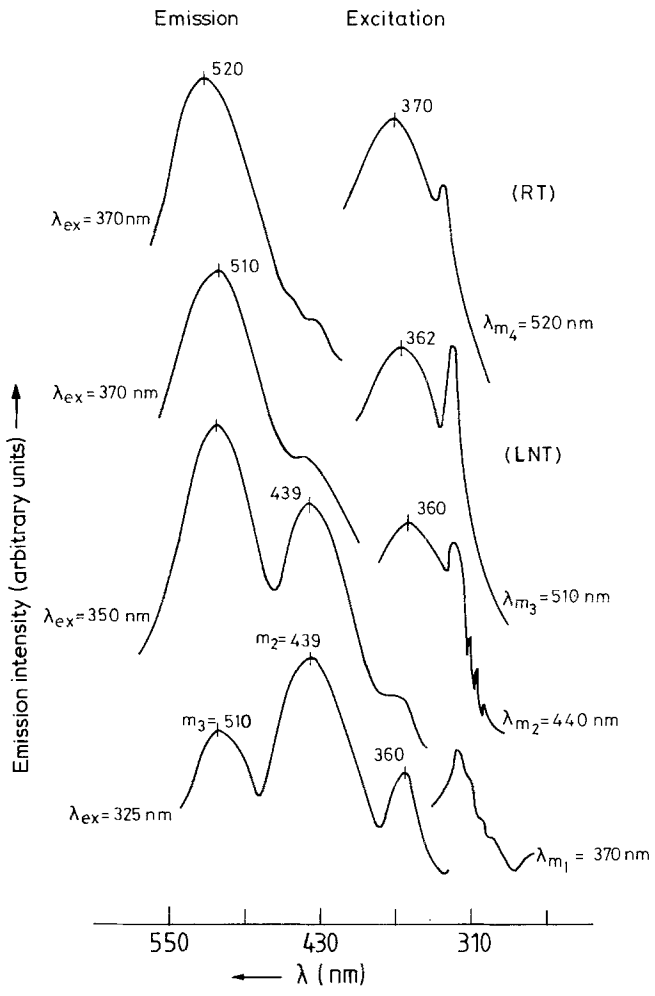

Figure 10 Emission and excitation spectra for $Zn_{0.85}Mg_{0.15}S:10^{-4}Cu,10^{-4}Br$ at $-196°C$. The top most curves are at room temperature.

change when the excitation wavelength is varied from 320 to 410 nm. The excitation spectrum of $Zn_{0.85}Mg_{0.15}S$:0.3Cu,0.35Br, with the monitored wavelength at 432 nm shows two bands, a comparatively broad band with maximum at 352 nm and another intense band with peak maximum at 319 nm. The latter is also observed in the excitation spectra of self-activated $Zn_{1-x}Mg_xS$ [31]. In the lattice absorption band region of the excitation spectra, there are three dips of low intensity corresponding to the excitation absorption. These dips appear around 314, 312 and 304 nm at low temperatures. They correspond to A_1, B_1 and C_1 exciton lines observed for 2H ZnS, with appropriate blue shift due to solid solution formation [32]. When the monitored wavelength is increased to 475 nm, the exciton band region of the excitation spectrum has higher intensity of absorption with the absence of the exciton dips. The absence of exciton absorption at higher monitoring wavelengths is a feature contrary to what is reported for 2H ZnS [32]. However, the spectra reported in [32] are with very low copper contents.

Hence, the PL spectra of $Zn_{0.85}Mg_{0.15}S:10^{-4}Cu,-10^{-4}Br$ were investigated. These studies have no relevance to EL phosphors since they are poorly electroluminescent. Fig. 10 shows the emission and excitation spectra at $-196°C$. The emission spectrum, with the excitation wavelength at 325 nm, has three bands. The maximum at 510 nm is the copper-green band [33–35]; the peak around 439 nm corresponds to the copper-blue [36–38], whereas the band around 362 nm is known to be due to the self-activated (SA) emission [39]. The wavelength maximum of the emission spectrum is a function of the excitation wavelength. The intensities of the emission spectra in Fig. 10 are one to two orders of magnitude lower than those in Fig. 9. As the excitation wavelength is increased from 325 to 350 nm, the intensity of the copper-blue emission decreases whereas that of the copper-green band increases; the SA emission band disappears. With further increase in excitation wavelength to 370 nm, the copper-blue becomes weaker and when $\lambda_{ex} = 400$ nm, only the green band persists. The copper-blue PL emission maximum shifts from 432 to 439 nm when copper concentration is lowered from 0.3 to 10^{-4} mol %. The possibility that the 439 nm emission band of $Zn_{0.85}Mg_{0.15}S:10^{-4}Cu,-10^{-4}Br$ may be associated with the SA emission is ruled out as we studied the SA emission behaviour of $Zn_{1-x}Mg_xS$ and found no emission band around 439 nm with or without intentional addition of bromine, aluminium or gallium [32]. Incorporation of copper alone gives rise to the 439 nm band. Addition of cationic donors like aluminium or gallium does not shift the 439 nm band whereas the SA emission shifts to longer wavelength under this treatment [31]. On cooling to liquid N_2 temperature, the 439 nm band is shifted to shorter wavelength with the half-band width remaining unchanged. Again, this trend is opposite to that for SA emission [31]. The disappearence of the SA emission peak at 362 nm, on increasing the excitation wavelength from 325 to 350 nm, is also noticed in

hexagonal ZnS:10^{-5}Cu by Hoshina and Kawai [32] which they explained to indicate the transfer of energy from the SA centre to the copper-blue centre.

The excitation spectrum of $Zn_{0.85}Mg_{0.15}S:10^{-4}Cu,-10^{-4}Br$ changes with the monitoring wavelength. When $\lambda_m = 510$ nm, the characteristic broad band appears with a maximum around 360 nm, accompanied by the higher energy band around 326 nm. When the monitoring wavelength is changed to 440 nm, the 326 nm band acquires higher intensity, accompanied by the appearance of the exciton absorption dips (of higher intensity than in Fig. 9), whose positions remain unchanged as in high copper-containing phosphor. With $\lambda_m = 370$ nm, only the high energy band persists, with peak maximum at 320 nm, together with the less defined exciton absorption dips.

Variation in bromine concentration in the range of 10^{-4} (intentionally added concentration which is over and above the background impurity content) to 0.35 mol %, at fixed copper contents showed no effect on the PL spectra.

4. Discussion

Luminescence characteristics of the crystallophosphors have to be viewed in the light of the crystal structure changes. Smith [19] has reported a contraction of ZnS unit cells by the incorporation of magnesium. The present results as well as those of previous authors [12, 18] show that the lattice parameters increase with magnesium content in $Zn_{1-x}Mg_xS$. The ion sizes of Zn^{2+} and Mg^{2+} are 0.06 and 0.058 nm respectively for 4-coordination [40]. Accordingly, a reverse trend should be expected on the basis of an ionic model. However, ZnS can be better described on the basis of a covalent model, in which the percentage ionicity of the metal–sulphur band is increased by the replacement of zinc by the more electropositive alkaline earth metal, magnesium. Thereby, the wurtzite, rather than zinc blende, structure is stabilized. Dehesa *et al.* [41] have shown that the difference in stabilization energy between these two type-structures, for a given compound, is mainly electrostatic in character. Substitutional impurities which contribute to electrostatic energy stabilize the wurtzite form. The transformation is continuous with impurity concentration, as evident from Fig. 1.

Expansion of the lattice will decrease the energy gap, accompanied by a red shift in the emission as well as in the absorption spectrum [19, 20]. This statement does not hold good for $Zn_{1-x}Mg_xS$ where the lattice expansion is accompanied by increased E_g values (Fig. 8). The dependence of unit cell parameters (Fig. 2) as well as the E_g values on composition indicates that $Zn_{1-x}Mg_xS$ are non-ideal solid solutions. The emission spectral characteristics of copper-doped $Zn_{1-x}Mg_xS$ (Fig. 4) are also indicative of their non-ideal nature.

Luminescence spectra (both EL and PL) show that the copper-blue emission of ZnS:0.35Cu,0.3Br is always accompanied by the green emission band. Whereas for $Zn_{1-x}Mg_xS$:0.3Cu,0.3Br, the green band is absent when $x \geqslant 0.13$ and has the 2H structure. A few alternative explanations are possible for the disappearance of the green band:

(i) The fact that the change in luminescence spectrum is accompanied by the phase change to 100% hexagonal may indicate a change in symmetry of the copper-centre, as proposed by Birman [42]. Accordingly, copper-green and copper-blue emissions result from different states of the same centre which acquires the symmetry elements of the valence band of the corresponding host lattice.

(ii) The emission of the copper-centre may show a blue shift which follows the blue shift in the absorption edge due to magnesium incorporation. Such a situation has been recently reported for $Zn_{1-x}Mg_xTe$: Li which also shows lattice expansion upon solid solution formation [43].

(iii) Magnesium may function as an isoelectronic cation impurity centre [44]. The ionization energy of magnesium is smaller than that of zinc. Therefore, the effective charge on sulphide ions adjacent to Mg_{Zn} becomes more negative than that on normal lattice sites. Hence the energy of the valence electron around Mg_{Zn} tends to be higher than that of the normal valence electron. This generates a short-range potential attractive to holes near magnesium. The intrinsic exciton produced around Mg_{Zn} relaxes to a bound exciton, the recombination of which may transfer energy resonantly to the copper-centre thus modifying the emission spectrum of the latter. Modification of the hole binding energy of the SA centre, $(V_{Zn} - Br_S)$, by magnesium has been reported earlier [31].

(iv) Coupling between SA and copper-centres [45] can be modified by the presence of magnesium so that the resonance energy transfer to the blue centre is favoured.

(v) The increased electrostatic contribution to lattice stabilization energy accompanied by the lattice expansion may alter the chemical character of the copper-centre thereby changing the position of the corresponding energy levels.

Only explanation (v) above can account for the presence of both the green and the blue bands in the emission spectrum of $Zn_{0.85}Mg_{0.15}S:10^{-4}$Cu, Br and for the fact that, at larger excitation wavelength, only the green emission persists (Fig. 10). For this phosphor, the copper-blue and SA emissions accompanying the copper-green emission are indicative of the energy transfer from copper-blue and SA centres to the copper-green centre. Energy transfer also takes place from the SA centre to the copper-blue centre. These are the same characteristics reported for 2H ZnS containing 10^{-4} mol % Cu [32]. Whereas, with 0.3 mol % Cu, the blue emission is observed without the appearance of the SA band. This is indicative of the changing nature of the copper-centres with concentration. The widely accepted view is that the copper-green band originates from the electron-hole recombination at a distant donor (Br_S^+)–acceptor (Cu_{Zn}^-) pair (DA pair) [32–35]. Although there are many models for the copper-blue centre, the one in better agreement with the experimental results is the electron-hole recombination at a $(Cu_{Zn}^- Cu_i^+)$ pair and an isolated donor (DI pair) [36–38, 45]. The nearest

neighbour pair of Cu_{Zn}^{-} and an interstitial Cu^{+} ion is tightly bound to form a neutral isoelectronic centre, which can act as a hole trap, as mentioned earlier. The donor involved in such DI pair transition is Br_S^{+} whose actual concentration (relative to that of copper) does not affect the peak position of the copper-blue band in $Zn_{1-x}Mg_xS$. However, the emission spectrum is affected by the variation in copper-concentration, supporting the contention that the changing nature of the copper-centre causes the disappearance of the green band. It is possible that at higher copper concentrations, more Cu^{+} ions go into the interstitial positions so that more $(Cu_{Zn}^{-}Cu_i^{+})$ associated pairs are produced. We propose that in hexagonal $Zn_{1-x}Mg_xS$, the interstitial Cu^{+} is more prevalent than in ZnS particularly at higher copper contents. Therefore, the number of isolated Cu_{Zn}^{-} is low, causing the diminution in intensity of the green band. The predominance of Cu_i^{+} may arise from the changed crystallochemical characteristics of the host lattice as discussed earlier. It is known that an increased copper/bromine ratio in ZnS leads to the predominance of the blue band [46], possibly due to the presence of more $(Cu_{Zn}^{-}Cu_i^{+})$ associated pairs. The persistance of the green side band indicates that isolated Cu_{Zn}^{-} cannot be minimized in ZnS.

The exciton structures in the excitation spectra are related to the optical excitation mechanism of the corresponding centre. They will appear as peaks in the energy region near the band gap, depending upon whether the recombination energy of the bound exciton is transferred to the centre or as dips if the optically produced intrinsic excitons are non-radiatively annihilated at the recombination centre [47]. The excitons by the donor (Br_S^{+})–acceptor (Cu_{Zn}^{-}) pairs are of shorter distances [32]. Lower intensity of these exciton dips at higher copper concentration may suggest lower number of isolated Cu_{Zn}^{-} acceptors. The characteristic excitation band around 350 to 360 nm may be due to the ionization of electron from $(Cu_{Zn}^{-}\ Cu_i^{+})$ or Cu_{Zn}^{-} to the conduction band. Photoconduction is reported following excitation into these bands [48]. The band around 320 nm in the excitation spectra may involve the excitation of a valence band electron into the donor levels of isolated Br_S^{+}. This is supported by the presence of the 320 nm band in Br-doped $Zn_{1-x}Mg_xS$ [31]. Although the 320 nm band, characteristic of SA luminescence, is present in the excitation band of $Zn_{0.85}Mg_{0.15}S:0.3Cu,0.3Br$, the emission spectra do not show the SA band (~ 370 nm). This may be due to the absence of coupling between the SA centre and $(Cu_{Zn}^{-}Cu_i^{+})$ in $Zn_{1-x}Mg_xS$ with higher copper contents.

The frequency and voltage dependence of EL intensity of $Zn_{1-x}Mg_xS:Cu,Br$ is similar to that of ZnS phosphors. Therefore, it can be concluded that the excitation mechanism, under the electrical field, remains unaffected. However, our results do not yield any information as to whether impact ionization or carrier injection is the cause for excitation in EL powder phosphors.

Acknowledgements

Thanks are due to the Humboldt Foundation for a fellowship which enabled T. R. N. Kutty to work in the University of Dortmund, West Germany, and to Professor A. G. Fischer for useful discussions during the early part of this work. Thanks are also due to C. S. I. R., New Delhi, for a research scholarship to R. Revathi.

References

1. G. DESTRIAU, *J. Chim. Phys.* **30** (1936) S620.
2. S. ROBERTS, *J. Appl. Phys.* **28** (1957) 262.
3. W. A. THORNTON, *J. Electrochem. Soc.* **107** (1960) 895.
4. W. LEHMANN, *ibid.* **113** (1966) 40.
5. *Idem, J. Electronic. Mater.* **11** (1982) 391.
6. S. M. PILLAI and C. P. G. VALLABHAN, *Solid State Commun.* **47** (1983) 909.
7. W. LEHMANN, *J. Electrochem. Soc.* **110** (1963) 754.
8. A. G. FISCHER, K. KOEGER, D. HERBST and J. KNUFFER, in Proceedings of the 3rd European Electro-optics Conference, *Soc. Photo-Opt. Inst. Engrs.* **99** (1976) 202.
9. Y. MAKANISHI and Y. YAMASHITA, *Appl. Phys. C.* **20** (1981) 2261.
10. P. M. JAFFE, *J. Electrochem. Soc.* **110** (1963) 979.
11. A. G. FISCHER, *Nach. Tech. Zeitung.* **33** (1980) 162.
12. L. A. SYSOEV and N. F. OBUKHOVA, *Monokhrist. Tekh.* **10** (1974) 20.
13. N. F. OBUKHOVA, L. V. ATROSCHENKO and A. I. KOLODYAZHNYI, *Izv. Akad. Nauk SSSR Neorg. Mater.* **13** (1977) 1390.
14. A. E. NOVIK, E. V. PERNITSKII, A. E. RYSKIN, L. A. SYSOEV and G. E. KHIL'KO, *Fiz. Tverd. Tela.* **16** (1974) 1147.
15. I. M. SIL'VESTROVA, N. F. OBUKHOVA, L. V. ATROSCHENKO, L. A. SYSOEV and YU. V. PISAREVSKII, *Izv. Akad. Nauk SSSR Neorg. Mater.* **14** (1978) 1031.
16. D. L. FEDOROV, L. G. SUSLINA and A. G. ARESHKIN, *Fiz. Tverd. Tela.* **24** (1982) 821.
17. YU. D. KONDRASHCHEV and TU. A. OMEL'CHENKO, *Z. Neorgan. Khim.* **9** (1964) 937.
18. J. W. BRIGHTWELL, B. RAY and S. WHITE, *J. Mater. Sci. Lett.* **3** (1984) 951.
19. A. I. SMITH, *J. Electrochem. Soc.* **99** (1952) 155.
20. F. A. KROEGER, *J. Opt. Soc. Amer.* **39** (1949) 670.
21. T. W. SARGE, US Patent 2358 661, (1944).
22. B. J. SKINNER and B. B. BARTON, *Amer. Mineral.* **45** (1960) 612.
23. M. AVEN and J. A. PARODI, *J. Phys. Chem. Solids.* **13** (1966) 56.
24. R. C. WEAST (Ed) in "Hand Book of Chemistry and Physics" 59th Edn. (CRC Press Inc, Cleveland, Ohio, 1978) p. E101.
25. National Bureau of Standards Circulars **539 7** (1957) 31 and **539 2** (1953) 14.
26. G. BERTHOLD, *Z. Phys.* **181** (1964) 333.
27. T. P. McCLEAN in "Progress in Semiconductors 5" edited by A. F. Gilson (Heywood and Co. Ltd., London, 1960) pp. 55-101.
28. W. W. WENDLANDT and H. G. HECHT "Reflectance Spectroscopy" (Interscience, New York, 1966) p. 54.
29. B. RAY, "II–VI Compounds" (Pergamon, London, 1969) p. 54.
30. S. SHIONOYA in "Luminescence of Inorganic Compounds" edited by P. Goldberg, (Academic Press, New York, 1966) p. 244.
31. T. R. N. KUTTY and R. REVATHI, *Solid State Commun.* **55** (1985) 197.
32. T. HOSHINA and H. KAWAI, *Jpn. J. Appl. Phys.* **19** (1980) 267, 279.
33. J. S. PRENER and F. E. WILLIAMS, *J. Electrochem. Soc.* **103** (1956) 342.
34. E. F. APPLE and F. E. WILLIAMS, *ibid.* **106** (1959) 224.
35. K. ERA, S. SHIONOYA and Y. WASHIZAWA, *J. Phys. Chem. Solids* **29** (1968) 1827, 1843.

36. H. BLICKS, N. RIEL and R. SIZMANN, *Z. Phys.* **163** (1961) 594.
37. W. RIEL and R. SIZMANN, in "Luminescence in organic and inorganic materials" edited by H. P. Kallmann and G. H. Spruch, (John Wiley, New York 1962) p. 344.
38. K. URABE, S. SHIONOYA and A. SUZUKI, *J. Phys. Soc. Jpn.* **25** (1968) 1611.
39. S. ROTHSCHILD, *J. Electrochem. Soc.*, **110** (1963) 28.
40. R. D. SHANNON and C. T. PREWITT, *Acta. Crystallogr.* **B26** (1970) 1046.
41. J. S. DEHESA, J. A. VERGES' and C. TEJEDOR, *Solid State Commun.* **38** (1981) 871.
42. J. L. BIRMAN, *J. Electrochem. Soc.* **107** (1960) 409.
43. S. DEMIAN, F. EL. EKKAD, B. FARAG, H. MATHIEU, M. ROUZEYRE and J. CHEVALLIER, *Phys. Status Solidi.* **81** (2) (1984) 549.
44. J. J. HOPFIELD, D. G. THOMAS and R. T. LYNCH, *Phys. Rev. Lett.* **17** (1966) 312.
45. A. E. THOMAS, G. J. RUSSEL and J. WOODS, *J. Phys. C.* **17** (1984) 6219.
46. W. VAN GOOL, *Philips. Res. Repts. Suppl.* **3** (1961) 1.
47. H. KAWAI and T. HOSHINA, *Solid State Commun.* **22** (1977) 391.
48. I. BROSER and H. J. SCHULZ, *J. Electrochem. Soc.* **108** (1961) 545.

Received 1 May
and accepted 14 August 1985